

# Addressing Cosmological Tensions by Non-Local Gravity

Filippo Bouché <sup>1</sup> , Salvatore Capozziello <sup>1,2,3,\*</sup>  and Vincenzo Salzano <sup>4</sup> 

<sup>1</sup> Scuola Superiore Meridionale, Largo S. Marcellino 10, I-80138 Napoli, Italy

<sup>2</sup> Dipartimento di Fisica “E. Pancini”, Università di Napoli “Federico II”, Via Cinthia 21, I-80126 Napoli, Italy

<sup>3</sup> Istituto Nazionale di Fisica Nucleare, Sez. di Napoli, Via Cinthia 21, I-80126 Napoli, Italy

<sup>4</sup> Institute of Physics, University of Szczecin, Wielkopolska 15, 70-451 Szczecin, Poland

\* Correspondence: capozziello@na.infn.it

**Abstract:** Alternative cosmological models have been under deep scrutiny in recent years, aiming to address the main shortcomings of the  $\Lambda$ CDM model. Moreover, as the accuracy of cosmological surveys improved, new tensions have risen between the model-dependent analysis of the Cosmic Microwave Background and lower redshift probes. Within this framework, we review two quantum-inspired non-locally extended theories of gravity, whose main cosmological feature is a geometrically driven accelerated expansion. The models are especially investigated in light of the Hubble and growth tension, and promising features emerge for the Deser–Woodard one. On the one hand, the cosmological analysis of the phenomenological formulation of the model shows a lowered growth of structures but an equivalent background with respect to  $\Lambda$ CDM. On the other hand, the study of the lensing features at the galaxy cluster scale of a new formulation of non-local cosmology, based on Noether symmetries, makes room for the possibility of alleviating both the  $H_0$  and  $\sigma_8$  tension. However, the urgent need for a screening mechanism arises for this non-local theory of gravity.

**Keywords:** Hubble tension; growth tension; dark energy; alternative cosmological models; non-local gravity; Noether symmetries; galaxy clusters; elliptical galaxies; S2 star; gravitational waves



**Citation:** Bouché, F.; Capozziello, S.; Salzano, V. Addressing Cosmological Tensions by Non-Local Gravity. *Universe* **2023**, *9*, 27. <https://doi.org/10.3390/universe9010027>

Academic Editor: Yungui Gong

Received: 3 December 2022

Revised: 24 December 2022

Accepted: 25 December 2022

Published: 30 December 2022



**Copyright:** © 2022 by the authors. Licensee MDPI, Basel, Switzerland. This article is an open access article distributed under the terms and conditions of the Creative Commons Attribution (CC BY) license (<https://creativecommons.org/licenses/by/4.0/>).

## 1. Introduction

Recent astrophysical and cosmological surveys, both from ground-based and space experiments, have provided extremely high-quality data. The observations point towards a Universe in which the cosmological principle holds on large scales, namely the Universe appears homogeneous and isotropic if averaged over scales of  $\sim 100 h^{-1} \text{Mpc}$  or more [1,2]. Moreover, the Universe is undergoing an accelerated expansion phase [3,4], subsequent to a decelerated era in which the structure formation occurred. All these features, together with the nuclei abundances produced in the Big Bang Nucleosynthesis (BBN), the Baryon Acoustic Oscillations (BAO) and many others, are well predicted by the Lambda Cold Dark Matter ( $\Lambda$ CDM) model, which has been adopted as the standard cosmological model accordingly. Such a model provides an effective description of the Universe, which relies on the assumption that General Relativity (GR) is the final theory of gravitation that governs the cosmic dynamics. As a consequence, two more fluids other than baryonic matter and radiation must be inserted in the matter–energy content of the Universe in order to adjust GR predictions to data: the Dark Energy (DE), responsible for the late time cosmic acceleration, and the Dark Matter (DM), which accounts for the structure formation. Together, they should represent  $\sim 95\%$  of the matter–energy budget of the Universe [5–7], thus dominating the cosmic dynamics at all scales.

Building on its capability to fit the whole cosmological and astrophysical dataset with a relatively small number of parameters, the  $\Lambda$ CDM model stands as the pillar of our comprehension of the Universe. However, several shortcomings [8] and recently risen tensions [9–11] affect its reliability. On the one hand, we have a huge assortment of candidates but no final solution for DM [12,13] and DE [14–16]. On the other hand, the presence

of singularities, as well as the inconsistency at quantum level, undermine the credibility of GR as the final theory of gravity. Even more puzzling are the cosmological tensions, which have emerged in recent years as the result of the growing availability of a wide range of extremely precise data. A multitude of independent observations appears indeed to be in a  $\gtrsim 2\sigma$  tension with the reference  $\Lambda$ CDM estimates by the Planck collaboration [5]. Even though systematic experimental errors may account for part of these tensions, their statistical significance and their persistence after several check analyses have thrown up some serious red flags. Since the Planck constraints for the cosmological parameters relies on a strongly  $\Lambda$ CDM-model-dependent analysis of the Cosmic Microwave Background (CMB), such tensions may be the signature of the breakdown of the concordance model, hence of new physics. In this paper, we pay particular attention to the two most well-known tensions: the  $H_0$  tension [10], which emerges from the comparison between early-time [5] and late-time measurements [17] of the Hubble constant, and the growth tension [11] between the CMB value [5] of the cosmological parameters  $\Omega_M$  and  $\sigma_8$  and those from lower redshift probes, such as Weak Lensing (WL) [18], Cluster Counts (CC) [19] and Redshift Space Distortion (RSD) [20].

In order to meet the challenges posed by  $\Lambda$ CDM theoretical shortcomings, as well as by its observational tensions, a zoo of alternative cosmological models has been formulated in recent years. The common feature of any proposed model is the introduction of additional degrees of freedom, whether in the gravitational or the matter–energy Lagrangian. Several approaches have been adopted: from the simple generalization of the Hilbert–Einstein action to functions of the curvature scalar, namely  $f(R)$  theories [21–27], to the addition of further geometric invariants such as the torsion scalar  $T$  [27–32] or the Gauss–Bonnet scalar  $\mathcal{G}$  [33–36]. The introduction of scalar/vector fields minimally or non-minimally coupled to gravity [37–41], as well as the emergence of non-trivial dynamics in the dark sector [42–46], also represent intriguing possibilities in the extremely wide framework of the alternatives to GR/ $\Lambda$ CDM (see [47,48] for the state of the art). In this paper, we want to inquire into a specific class of alternative cosmological models ruled by non-local gravitational interactions [49]. Among others, we investigate the cosmological implications of two non-locally extended theories of gravity: the Deser–Woodard (DW) model [50] and the Ricci-Transverse (RT) model [51]. These theories have drawn increasing attention in recent years due to their capability to account for late-time cosmic acceleration, thus avoiding the introduction of any form of unknown dark energy. Moreover, the non-local corrections may provide a viable mechanism to alleviate some of the main cosmological tensions.

The paper is organized as follow: in Section 2, we outline the main motives for formulating non-local theories of gravity, and we present the two ways in which dynamical non-locality can be implemented. Then, we introduce the two chosen models and their theoretical features. In Section 3, we investigate the mechanisms through which the DW and the RT model account for the accelerated expansion of the Universe. In Section 4, we present the non-locally driven evolution of cosmological perturbations for the two models and the resulting impact on the  $\sigma_8$  tension. Moreover, in Section 5, we assess the  $H_0$  tension in light of the non-local theories. Finally, in Section 6, we present the main astrophysical tests of the non-local gravity models. The conclusions are drawn in Section 7.

## 2. Non-Local Gravity

Non-locality naturally emerges in Quantum Physics, both as a kinematical and a dynamical feature. On the other hand, locality is a key property of classical field theories, and thus represents one of the main obstacles to overcome in order to merge gravitational interaction formalism with that of Quantum Field Theory (QFT). As a consequence, the introduction of non-locality in our theory of gravitation seems to be an unavoidable step towards the unification of the fundamental interactions. There exist at least two ways to achieve non-locality: at fundamental level, in which kinematical non-locality can be implemented by discretizing spacetime and introducing a minimal length scale (usually the Planck length); as an effective approach, in which non-local geometrical operators can

be added to the gravitational Lagrangian to obtain a non-local dynamics in a continuum background spacetime [52]. Here, we want to focus on the latter scenario, which is of great interest for cosmological applications.

Two main classes of non-locally extended theories of gravity have been developed in recent years [49]: Infinite Derivative theories of Gravity (IDGs), involving entire analytic transcendental functions of a differential operator, and Integral Kernel theories of Gravity (IKGs) based on integral kernels of differential operators, such as

$$\square^{-1}R(x) = \int d^4x' G(x, x')R(x'), \tag{1}$$

where  $G(x'x')$  is the Green function associated to the inverse d'Alembertian. IDGs usually address the ultraviolet (UV) problems of the  $\Lambda$ CDM model by ensuring classical asymptotic freedom. The gravitational interaction is weakened on small scales and the singularities disappear accordingly. Non-singular black holes [53], as well as inflationary [54] and bouncing cosmologies [55], are indeed forecast in the IDG framework. On the other hand, IKGs are introduced to account for the infrared (IR) shortcomings of the concordance model of cosmology. The phenomenology of both dark fluids can be actually reproduced by non-local corrections that switch on at large scales [50,56,57].

In this paper, we focus on two specific curvature-based IKGs [50,51] and their cosmological features. IKGs indeed have special relevance due to the fact that they combine suitable cosmological behavior with well-justified Lagrangians at the fundamental level. GR is actually plagued by quantum IR divergences that already appear for pure gravity in flat space [58]. This pathological behavior implies that the long-range dynamics of the gravitational interaction may be non-trivial, and non-perturbative techniques are thus required. Applying such non-perturbative methods to the renormalization of the quantum effective action of the gravity theory, non-local terms emerge both associated [59,60] or not associated [61,62] to a dynamical mass scale. Analogous results can be recovered through the trace anomaly [63].

### 2.1. The Deser–Woodard Model

The first model that we want to highlight is an IKG initially proposed in [50]. The non-locally extended gravitational action of the Deser–Woodard model reads

$$S = \frac{1}{16\pi G} \int d^4x \sqrt{-g} \left\{ R[1 + f(\square^{-1}R)] \right\}, \tag{2}$$

where the non-local correction is given by the so-called distortion function, namely a general function of the inverse box of the Ricci scalar, as in Equation (1). It is worth noticing that the non-local theory reduces to GR as soon as  $f(\square^{-1}R)$  vanishes. The modified field equations descending from Equation (2) are

$$G_{\mu\nu} + \Delta G_{\mu\nu} = \kappa T_{\mu\nu}^{(m)}, \tag{3}$$

where the non-local correction reads

$$\begin{aligned} \Delta G_{\mu\nu} = & \left( G_{\mu\nu} + g_{\mu\nu}\square - \nabla_\mu \nabla_\nu \right) \left\{ f(\square^{-1}R) + \square^{-1} [Rf'(\square^{-1}R)] \right\} \\ & + \left[ \frac{1}{2} \left( \delta_\mu^\alpha \delta_\nu^\beta + \delta_\mu^\beta \delta_\nu^\alpha \right) - \frac{1}{2} g_{\mu\nu} g^{\alpha\beta} \right] \partial_\alpha (\square^{-1}R) \partial_\beta \left\{ \square^{-1} [Rf'(\square^{-1}R)] \right\}. \end{aligned} \tag{4}$$

Furthermore, the non-local gravitational action in Equation (2) can be easily rewritten under the standard of local scalar–tensor theories by introducing an auxiliary scalar field

$$R(x) = \square\eta(x), \tag{5}$$

which does not carry any independent degree of freedom. The local canonical form of the scalar–tensor action, equivalent to the non-local theory, thus reads [64]

$$S = \frac{1}{2\kappa} \int d^4x \sqrt{-g} \left\{ R[1 + f(\eta)] - \partial_\mu \zeta \partial^\mu \eta - \zeta R \right\}, \tag{6}$$

where  $\zeta(x)$  is a Lagrangian multiplier which has been promoted to a position- and time-dependent scalar field. In this formulation, the gravitational field equation is

$$G_{\mu\nu} = \frac{1}{1 + f(\eta) - \zeta} \left[ \kappa T_{\mu\nu}^{(m)} - \frac{1}{2} g_{\mu\nu} \partial^\alpha \zeta \partial_\alpha \eta + \frac{1}{2} (\partial_\mu \zeta \partial_\nu \eta + \partial_\mu \eta \partial_\nu \zeta) - (g_{\mu\nu} \square - \nabla_\mu \nabla_\nu) (f(\eta) - \zeta) \right], \tag{7}$$

while the Klein–Gordon equations for the two auxiliary scalar fields are

$$\square \eta = R, \tag{8}$$

$$\square \zeta = -R \frac{\partial f(\eta)}{\partial \eta}. \tag{9}$$

### 2.2. The Ricci-Transverse Model

The second non-local model that we investigate through this paper is a metric IKG proposed in [51]. This is a quantum-inspired model, whose quantum effective action is

$$\Gamma = \frac{1}{64\pi G} \int d^4x \left[ h_{\mu\nu} \mathcal{E}^{\mu\nu,\alpha\beta} h_{\alpha\beta} - \frac{2}{3} m^2 (P^{\mu\nu} h_{\mu\nu})^2 \right], \tag{10}$$

where  $g_{\mu\nu} = \eta_{\mu\nu} + \kappa h_{\mu\nu}$  is the linearized metric tensor,  $\mathcal{E}^{\mu\nu,\alpha\beta}$  is the Lichnerowicz operator<sup>1</sup>,  $P^{\mu\nu} = \eta^{\mu\nu} - (\partial^\mu \partial^\nu / \square)$  is a projector operator and  $m$  is the mass of the conformal mode of the gravitational field. Performing the covariantization of Equation (10), the modified gravitational field equation reads

$$G_{\mu\nu} - \frac{1}{3} m^2 (g_{\mu\nu} \square^{-1} R)^T = \kappa T_{\mu\nu}, \tag{11}$$

where we take the transverse part of the symmetric non-local tensor  $S_{\mu\nu} = g_{\mu\nu} \square^{-1} R$

$$S_{\mu\nu} = S_{\mu\nu}^T + \frac{1}{2} (\nabla_\mu S_\nu + \nabla_\nu S_\mu), \tag{12}$$

and  $S_\mu$  is an associated four-vector. The Bianchi identities are guaranteed accordingly, i.e.,  $\nabla^\mu S_{\mu\nu}^T = 0$ .

In the same way as the DW model, the Ricci-Transverse model can be localized through a scalar–tensor–vector formulation [51,65]. Here, we introduce two auxiliary objects, namely

$$U(x) = -\square^{-1} R(x), \quad \mathcal{S}_{\mu\nu}(x) = -U(x) g_{\mu\nu}(x) = g_{\mu\nu}(x) \square^{-1} R(x). \tag{13}$$

An auxiliary four-vector field  $S_\mu(x)$  therefore enters the localized equations because of Equation (12). The gravitational field equation, Equation (11), turns into

$$G_{\mu\nu} + \frac{m^2}{6} (2U g_{\mu\nu} + \nabla_\mu S_\nu + \nabla_\nu S_\mu) = \kappa T_{\mu\nu} \tag{14}$$

plus the two equations of motions of the two auxiliary fields

$$\square U = -R, \tag{15}$$

$$(\delta_\nu^\mu \square + \nabla^\mu \nabla_\nu) \mathcal{S}_\mu = -2\partial_\nu U. \tag{16}$$

### 3. The Late-Time Cosmic Acceleration

The Universe is currently undergoing an accelerated expansion. The first evidence of this peculiar behavior dates back to the end of the twentieth century, when the observation of several Type Ia Supernovae (SNIa) [3,4] pointed out the unavoidable necessity of a cosmological constant to fit the cosmic expansion history. On the one hand, these results have been corroborated by the observations of all the recent surveys [5,66–68]. On the other hand, the theoretical explanation of this issue has two main drawbacks: the fine tuning problem [69] and the coincidence problem [70]. The former is related to the huge discrepancy (~120 orders of magnitude) between the observed value of the cosmological constant and the vacuum energy density calculated via QFT. The latter is linked with the similar current values of  $\Omega_\Lambda$  and  $\Omega_{M,}$  despite their radically different evolution laws.

The next generation of cosmological surveys should boost the investigation of the nature of the so-called cosmological constant, providing powerful data to discriminate between DE solutions and extended theories of gravity. Within this framework, non-local gravity provides viable mechanisms that could account for the observed accelerated expansion of the Universe.

#### 3.1. The DW Case: Delayed Response to Cosmic Events

The main reason why the DW model has been in the spotlight since its formulation is its effective way to explain late-time cosmic acceleration without the introduction of any form of dark energy. Computing the non-local correction of Equation (2) in the Friedmann–Lemaître–Robertson–Walker (FLRW) metric,

$$ds^2 = -dt^2 + a^2(t)d\vec{x} \cdot d\vec{x}, \tag{17}$$

one obtains a non-negligible geometrical contribution,

$$\begin{aligned} [\square^{-1}R](t) &= \int_0^t dt' \frac{1}{a^3(t')} \int_0^{t'} dt'' a^3(t'') R(t'') \\ &= -\frac{6s(2s-1)}{3s-1} \left[ \ln\left(\frac{t}{t_{eq}}\right) - \frac{1}{3s-1} + \frac{1}{3s-1} \left(\frac{t_{eq}}{t}\right)^{3s-1} \right], \end{aligned} \tag{18}$$

where  $a(t) \sim t^s$ , and the integration constant is set to make the non-local correction vanish before the radiation–matter equivalence time,  $t_{eq}$ . Then, for  $t > t_{eq}$  the non-local correction starts to grow, becoming non-negligible at late time and driving the accelerated cosmic expansion. Non-locality thus emerges in the cosmological framework as a delayed response to the radiation-to-matter dominance transition, i.e., as a time-like non-local effect.

The introduction of non-locality may therefore have beneficial effects on cosmological scales, both at background level and perturbations level. Two different approaches can be adopted for the DW model: on the one hand, one can exploit the freedom guaranteed by the undetermined form of the distortion function to fit the observed expansion history of the universe. In such a scenario, the DW cosmology is made equivalent to  $\Lambda$ CDM at the background level. However, different features emerge when perturbations are taken into account, and the physics of structure formation is affected accordingly. On the other hand, one can select the form of the distortion function building on some fundamental principles, such as the Noether symmetries of the system. In this case, the non-local cosmology is also modified at background level and stronger deviations from the concordance model should rise.

In [71], the first method has been applied, and the  $\Lambda$ CDM expansion history of the Universe has been accurately reproduced by matching the data through a non-trivial form of the distortion function

$$f(\square^{-1}R) = 0.245 [\tanh(0.350X + 0.032X^2 + 0.003X^3) - 1], \tag{19}$$

where  $X = \square^{-1}R + 16.5$ .

### 3.2. The RT Case: Dynamical Dark Energy

Considering a spatially flat FLRW metric, Equation (17), the equations of motion of the RT model, Equations (14)–(16), become [72]

$$H^2 - \frac{m^2}{9}(U - \dot{S}_0) = \frac{8\pi G}{3}\rho, \tag{20}$$

$$\ddot{U} + 3H\dot{U} = 6\dot{H} + 12H^2, \tag{21}$$

$$\ddot{S}_0 + 3H\dot{S}_0 - 3H^2S_0 = \dot{U}, \tag{22}$$

where the spatial components of the vector field  $S_\mu$  vanish to preserve the rotational invariance of the FLRW metric, and the stress–energy tensor is taken to be  $T_\nu^\mu = \text{diag}(-\rho, p, p, p)$ . Defining  $Y = U - \dot{S}_0$ ,  $\tilde{h} = H/H_0$  and the dimensionless variable  $x \equiv \ln a(t)$ , then the modified Friedmann equation, Equation (20), reads

$$\tilde{h}^2(x) = \Omega_M e^{-3x} + \gamma Y(x), \tag{23}$$

with  $\gamma \equiv m^2/(9H_0^2)$ . An effective dark energy thus appears

$$\rho_{DE}(t) = \rho_0 \gamma Y(t), \tag{24}$$

where  $\rho_0 = 3H_0^2/(8\pi G)$ . Once the initial conditions for the auxiliary fields are set (see [56] for details), the evolution of  $\rho_{DE}(t)/\rho_{TOT}(t)$  can be studied: the non-local effective dark energy is actually negligible until recent time and then starts to dominate the cosmic expansion. Moreover, it is possible to study the DE equation of state

$$\dot{\rho}_{DE} + 3H(1 + \omega_{DE})\rho_{DE} = 0, \tag{25}$$

and different evolutions for  $\rho_{DE}(z)$  follow from different choices for the initial conditions of the auxiliary fields. For small values of the initial conditions, one obtains a fully phantom DE, namely  $\omega_{DE}(z)$  is always less than  $-1$ . For large values of the initial conditions,  $\rho_{DE}(z)$  has a "phantom crossing" behavior, i.e., there is a transition from the phantom regime to  $-1 < \omega_{DE} < 0$  of about  $z \simeq 0.3$ . Regardless of the initial conditions, therefore, the non-local model provides a dynamical DE density which drives the accelerated expansion of the Universe.

## 4. The Growth of Perturbations and the $\sigma_8$ Tension

Building on the primordial density fluctuations emerged from the inflation, cosmic structures have formed due to gravitational instability. Studying the large-scale structure of the Universe and its evolution through the cosmic epochs, it is possible to trace the growth of the so-called cosmological perturbations.

Associated to this observable, one of the main cosmological tensions has risen: the growth tension. It has come about as the result of the discrepancy between the Planck value of the cosmological parameters  $\Omega_M$  and  $\sigma_8$  and those from WL measurements, CC and RSD data. The former dynamical probes point towards lower values of the amplitude ( $\sigma_8$ ) or the rate ( $f\sigma_8 = [\Omega_M(z = 0)]^{0.55}\sigma_8$ ) of growth of structures with respect to the CMB experiments, giving rise to a  $2 - 3\sigma$  tension [9,11]. Moreover, the Planck 2018 value of the joint parameter  $S_8 = \sigma_8\sqrt{\Omega_M/0.3}$  ( $S_8 = 0.834 \pm 0.016$  [5]) is confirmed by another recent CMB analysis by the ACT + WMAP collaboration ( $S_8 = 0.840 \pm 0.030$  [66]), thus erasing the possibility of a systematic error related to the excess of lensing amplitude measured by Planck [73].

A  $2.3\sigma$  tension emerges accordingly with both the original WL analysis of KiDS-450 [74] and KiDS-450 + VIKING data [75], while updated constraints from the same datasets [76,77] show greater discrepancies. The same  $2.3\sigma$  tension also occurs with the data from DES’s first year release (DESY1) [78], while the combination of KiDS-450 + VIKING + DESY1 weak lensing datasets results in a  $2.5\sigma$  [79] or  $3.2\sigma$  [80] tension depending on the analysis. The most recent cosmic shear data release from both KiDS-1000 and DESY3 confirms the previous estimates [18,81–84] ( $S_8 = 0.759^{+0.024}_{-0.021}$  from KiDS-1000 [18]). Analogous results have been obtained with the  $3 \times 2$  pt correlation function analysis (cosmic shear correlation function, galaxy clustering angular auto-correlation function and galaxy–galaxy lensing cross-correlation function) of KiDS-1000 + BOSS + 2dFLenS dataset [85]. Additional results, in agreement with those from WL surveys, have been achieved by number counting of galaxy clusters, using multiwavelength datasets [19,86–91]. Supplementary observational evidence for the weaker growth of structures is also given by the exploitation of RSD data [20,92–95].

#### 4.1. The Deser–Woodard Evolution of Scalar Perturbations

To investigate the growth of structures in the non-local DW model, we select the phenomenological form of the distortion function given by Equation (19). As a consequence, the non-local background evolution is made equivalent to that of  $\Lambda$ CDM, and any deviation is enclosed in the cosmological perturbations.

Consider the field equations of the scalar–tensor equivalent of the DW model, Equations (7)–(9). Specializing to the cosmological case by assuming the FLRW metric, Equation (17), the field equations now read

$$H^2 [1 + f - \xi] + H [f' \dot{\eta} - \dot{\xi}] - \frac{1}{6} \dot{\eta} \dot{\xi} = \frac{8\pi G}{3} \rho, \tag{26}$$

$$\dot{H} [1 + f - \xi] - \frac{H}{2} [f' \dot{\eta} - \dot{\xi}] + \frac{1}{2} \dot{\eta} \dot{\xi} + \frac{1}{2} [f'' \dot{\eta}^2 + f' \dot{\eta} - \dot{\xi}] = -4\pi G (p + \rho), \tag{27}$$

$$\ddot{\eta} + 3H\dot{\eta} = -6(\dot{H} + 2H^2), \tag{28}$$

$$\ddot{\xi} + 3H\dot{\xi} = 6f'(\dot{H} + 2H^2), \tag{29}$$

where the former two are the (0,0) and the (1,1) component of Equation (7), while the latter two are the cosmological formulation of Equations (8) and (9).

The linear perturbation equations have been derived in [96] for the scalar–tensor equivalent of the non-local theory, and then analogous results have been found in [97] for the original formulation. Using the perturbed FLRW metric in the Newtonian gauge,

$$ds^2 = -(1 + 2\Psi)dt^2 + a^2(t)(1 + 2\Phi)\delta_{ij}dx^i dx^j, \tag{30}$$

the growth equation reads

$$\ddot{\delta}_M + (2 - \xi)\dot{\delta}_M = \frac{3H_0^2 [1 - \xi - 8f'(\eta) + f(\eta)] \Omega_M^0}{2a^3 H^2 [1 - \xi - 6f'(\eta) + f(\eta)] [1 + f(\eta) - \xi]} \delta_M, \tag{31}$$

where  $\delta_M = \delta\rho_M/\rho_M$  is the matter density perturbation in the sub-horizon limit.

Numerical results for the growth rate  $f\sigma_8 \equiv \sigma_8 \delta'_M / \delta_M$  have been obtained in [96] and [97] for both the formulations of the Deser–Woodard model, and good agreement with the Redshift Space Distortion (RSD) data has emerged ( $\sigma_8^{NL} = 0.78$ ). Moreover, when the DW cosmological parameters are inferred by matching the CMB data [98], a lower growth amplitude with respect to that of  $\Lambda$ CDM turns out. The non-local model thus alleviates the growth tension, predicting compatible values of  $\sigma_8$  both from Planck–CMB and the other dynamical probes, as shown in Figure 1.

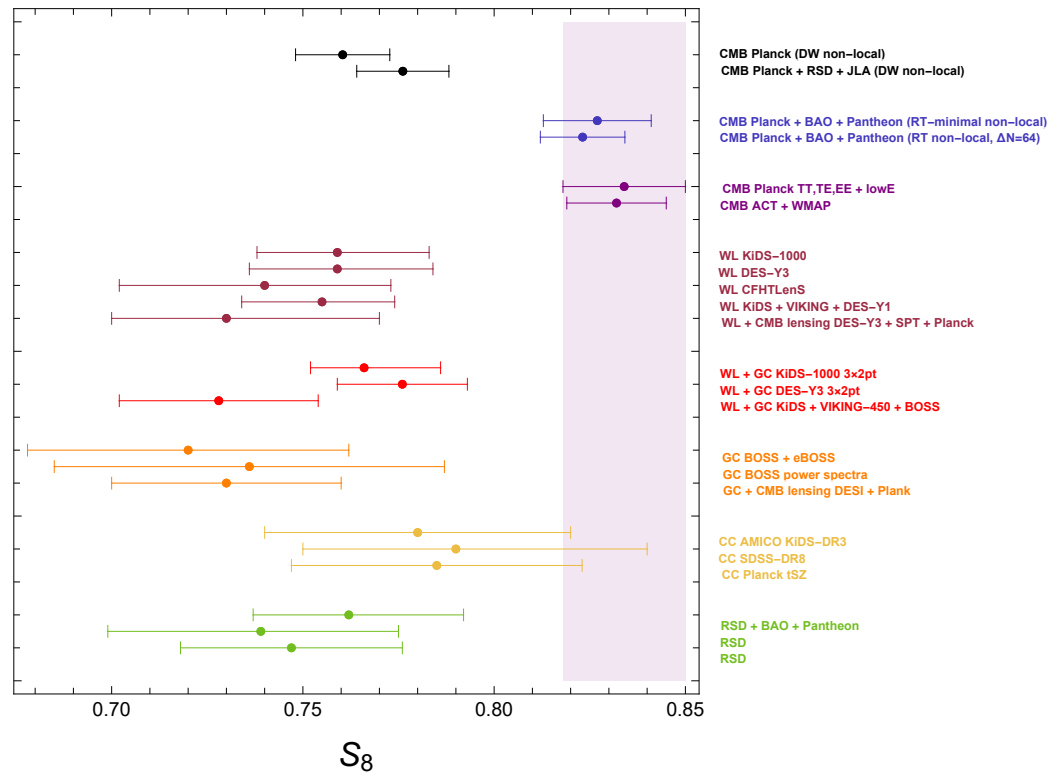


**Figure 1.** Estimates of  $S_8$  provided by the two non-local cosmological analyses [56,98], and the  $\Lambda$ CDM fit of the CMB [5,66], the WL data [18,20,80,83,84,99], the combination of WL and galaxy clustering observations [100–102], cluster counting [19,87,88] and RSD surveys [92,94]. The colored band corresponds to the  $S_8$  value derived by the analysis of the Planck–CMB data in the  $\Lambda$ CDM framework [5].

However, even though the non-local clustering of linear structures is weakened with respect to  $\Lambda$ CDM, and the DW prediction for the matter power spectrum is about 10% lower [98], the non-local lensing response is counterintuitively enhanced due to a severe increase in the lensing potential. This peculiar behavior results in a slight tension between CMB and RSD [98]: performing the joint fit, the RSD dataset tends to push the DW predictions for the CMB lensing potential  $C_\ell^{\phi\phi}$  out of the  $1\sigma$  error bars at low- $\ell$ . Applying the Bayesian tools for the model selection, a “weak evidence” [103] for the  $\Lambda$ CDM model consequently emerges.

#### 4.2. The Ricci-Transverse Evolution of Scalar Perturbations

The scalar perturbations of the RT model have been investigated in [56,104], using the FLRW metric in the Newtonian gauge, Equation (30), and perturbing the auxiliary fields as

$$U(t, \mathbf{x}) = \bar{U}(t) + \delta U(t, \mathbf{x}), \tag{32}$$

$$S_\mu(t, \mathbf{x}) = \bar{S}_0(t) + \delta S_\mu(t, \mathbf{x}) = \bar{S}_0(t) + \delta S_0(t, \mathbf{x}) + \partial_i [\delta S(t, \mathbf{x})], \tag{33}$$

where the spatial part of the vector perturbation does not vanish and, for scalar perturbations, only depends on  $\delta S$ . Building on the RT cosmological equations Equations (20)–(22), the growth equation for the matter density perturbation in the sub-horizon limit reads [104]

$$\ddot{\delta}_M + 2H\dot{\delta}_M = \frac{3}{2} \frac{G_{eff}}{G} H_0^2 \Omega_M \delta_M, \tag{34}$$

where in  $G_{eff}(\Psi, \Phi, \delta U, \delta S_0, S)$  is encoded the deviation of the non-local theory from GR. In the sub-horizon modes, namely  $\hat{k} \gg 1$ , such deviation is

$$1 - \frac{G_{eff}}{G} = \mathcal{O}\left(\frac{1}{\hat{k}^2}\right), \tag{35}$$

and the RT model is thus safe regarding the time variation of the effective Newton’s constant.  $G_{eff}$  indeed reduces to  $G$  at the Solar System scale, while a deviation of  $\sim 1\%$  rises at cosmological scales.

In [56], the growth rate  $f(z, k) \equiv d \ln \delta_M / d \ln a$  is also derived. The results do not differ from those of  $\Lambda$ CDM cosmology:  $f(z, k)$  can be fitted with a  $k$ -independent function  $f(z) = [\Omega_M(z)]^\gamma$ , where  $\gamma \simeq 0.55$  is roughly constant. Accordingly, any possible deviation in the growth of perturbations should be due to the amplitude  $\sigma_8$ . In order to find any signature of the non-local model at perturbation level, which could account for the growth tension, the theory was compared with cosmological observations: Planck–CMB, Pantheon SNIa and SDSS-BAO. The Bayesian parameter estimation shows a full equivalence between the RT non-local cosmology and the  $\Lambda$ CDM one. No statistically significant deviation in the  $\sigma_8$  parameter emerges for any of the tested versions of the Ricci-Transverse model. Eventually, this theory cannot alleviate the growth tension, as shown in Figure 1.

### 5. Hubble Tension in Light of the Non-Local Models

Hubble tension is certainly the most renowned and significant tension of the  $\Lambda$ CDM model. It emerges from the comparison between early-time and late-time measurements of the Hubble constant. From one side, CMB analysis [5,66,105–108], BAO surveys [6,101,109,110] with standard BBN constraints [111] and combinations of CMB, BAO, SNIa [112], RSD and cosmic shear data [78,113,114] point towards lower values of  $H_0$  ( $H_0 = 67.4 \pm 0.5 \text{ km s}^{-1}\text{Mpc}^{-1}$  from Planck 2018 [5]). On the other side, the local measurements based on standard candles prefer higher values for the Hubble constant [115] ( $H_0 = 73.04 \pm 1.04 \text{ km s}^{-1}\text{Mpc}^{-1}$  from SH0ES 2022 [17]). The main results are achieved by the SH0ES collaboration using Hubble Space Telescope observations: on the one hand, they analyzed SNIa data with distance calibration by Cepheid variables in the host galaxies [116,117]; on the other hand, they targeted long-period pulsating Cepheid variables [17,118], calibrating the geometric distance to the Large Magellanic Cloud, both from eclipsing binaries and parallaxes from the Gaia satellite [119,120]. Moreover, other independent local measurement of  $H_0$  have been performed by using time delays between multiple images of strong lensed quasars [121,122], the tip of the Red Giant Branch [123] and Miras (variable red giant stars) [124] with water megamaser as distance indicator [125]. All these measurements agree on higher values of the Hubble constant, thus generating a  $4 - 5\sigma$  tension with early-time model-dependent estimates.

#### 5.1. The Deser–Woodard Expansion History

The stat-of-the-art investigation of the DW non-local model does not allow any attempt to address  $H_0$  tension. To make the model predictive, the form of the distortion function needs to be specified, and most of the analyses have been focused on the phenomenological  $\Lambda$ CDM form of Equation (19), until now (see [98] for the latest results). This choice implies that the DW cosmology is made equivalent to that of the concordance model at background level, and the same expansion history, as well as the same  $H_0$ , are thus predicted (see Figure 2).

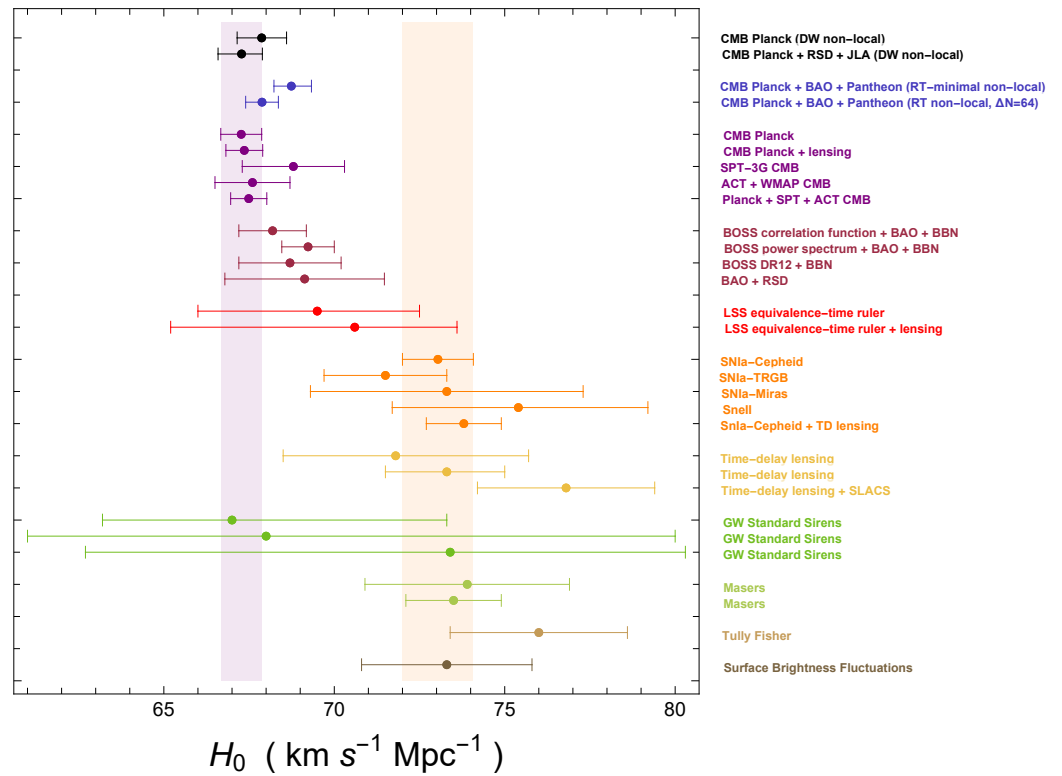


**Figure 2.** Estimates of  $H_0$  provided by the two non-local cosmological analyses [56,98], and the  $\Lambda$ CDM fit of the CMB [5,66,105,107], the matter power spectrum combined with BAO [20,110,126] and RSD [127], the Large Scale Structure  $t_{eq}$  standard ruler [128,129], the supernovae [17,121,124,130,131], the time-delay lensing [121,132,133], the gravitational waves [134–136], the water megamasers [125,137], the Tully–Fisher relation [138] and the SBF [139]. The colored bands correspond to the  $H_0$  estimates derived by the Planck–CMB analysis in the  $\Lambda$ CDM framework (purple) [5] and the SNIa–Cepheids analysis by SH0ES (orange) [17].

However, another option is also available for the selection of the distortion function. In [57,140,141], a specific form of  $f(\eta)$  has been derived by exploiting the Noether symmetries [142] of a spherically symmetric background spacetime

$$f(\eta) = 1 + e^\eta. \tag{36}$$

The accurate cosmological analysis of this form of the DW model has yet to be carried out, but some results have already been achieved, such as exact solutions [49] and a phase-space view of solutions [143]. Furthermore, several astrophysical tests have been performed on very different scales, and viable results turned out. In [141], the lensing properties of the galaxy clusters have been investigated in light of the exponential DW model, and a fully non-local regime with enhanced lensing strength has been highlighted. This feature clearly resembles the improved lensing response of the phenomenological form of the DW model, which is co-responsible for the lowered estimate of the  $\sigma_8$  parameter. A promising insight upon the cosmological behavior of the non-local theory based on Equation (36) thus emerges. Therefore, this model may alleviate not only the growth tension but also the Hubble tension, since it also deviates from GR at the background level [144]. Further analysis of the exponential DW model should be carried out accordingly.

### 5.2. The Ricci-Transverse Expansion History

For what concerns the RT model, the most updated cosmological analysis is due to Belgacem et al. [56]. As we saw in Section 4, different versions of the non-local model, relying on different choices for initial conditions of the auxiliary fields, have been compared

against Planck–CMB, Pantheon SNIa and SDSS-BAO data. Since the RT model has no freedom with regard to the functional form of the action, the theory cannot be adjusted to data, and no background equivalence to the  $\Lambda$ CDM cosmology can be established a priori. In such a scenario, the solution to the Hubble tension may thus be possible. However, the estimator tool defined in Equation (35), which accounts for the deviation from GR of the non-local theory, only shows little discrepancies. This manifests in the values of the cosmological parameters inferred via Markov Chain Monte Carlo (MCMC), which are almost equivalent to those of the concordance model. The only model that exhibits some slight discrepancies is the so-called "RT-minimal", which relies on the assumption that the auxiliary scalar field  $U(x)$  starts its evolution during the radiation dominance era. On the one hand, this model predict a non-vanishing value for the sum of neutrino masses, while the  $\Lambda$ CDM model and the other versions of the RT model show a marginalized posterior which is peaked in zero. On the other hand, the RT-minimal model provides a barely higher estimate of the Hubble constant, i.e.,  $H_0 = 68.74^{+0.59}_{-0.51} \text{ km s}^{-1} \text{ Mpc}^{-1}$ . Accordingly, the Hubble tension is just reduced to  $\sim 4\sigma$ , as shown in Figure 2.

The RT model in its minimal setup thus provides a viable mechanism to account for the late-time cosmic acceleration, as well as for the inclusion of non-zero neutrino masses. However, the predictions for both the background evolution and the linear perturbations are too similar to that of the  $\Lambda$ CDM model, hence the cosmological tensions cannot be alleviated.

### 6. Astrophysical Tests of Non-Local Gravity

As we saw, good cosmological behavior emerges for both of the non-local models, thus enabling the possibility to avoid the introduction of any form of unknown dark energy. In order to further investigate the viability of such models as alternatives to GR, it is then necessary to test the non-local predictions down to astrophysical scales. Moreover, an accurate investigation of the possible screening mechanisms should be performed, if necessary.

#### 6.1. Testing the Deser–Woodard Model by Galaxy Clusters, Elliptical Galaxies and the S2 Star

The DW model has been tested on a wide range of astrophysical scales, from the galaxy clusters [141] to the stellar orbits around Sagittarius A\* [140]. Most of the tests have been carried out for the exponential form of the non-local model, namely

$$S = \frac{1}{2\kappa} \int d^4x \sqrt{-g} \left[ R(2 + e^\eta) - \partial_\mu \zeta \partial^\mu \eta - \zeta R \right], \tag{37}$$

where the distortion function has been picked out by exploiting the Noether Symmetry Approach [145]. The analyses presented are all performed in the post-Newtonian limit, hence the non-local gravitational and metric potential are

$$\begin{aligned} \phi(r) = & -\frac{GM\eta_c}{r} + \frac{G^2M^2}{2c^2r^2} \left[ \frac{14}{9}\eta_c^2 + \frac{18r_\zeta - 11r_\eta}{6r_\eta r_\zeta} r \right] - \frac{G^3M^3}{2c^4r^3} \left[ \frac{50r_\zeta - 7r_\eta}{12r_\eta r_\zeta} \eta_c r \right. \\ & \left. + \frac{16}{27}\eta_c^3 - \frac{2r_\zeta^2 - r_\eta^2}{r_\eta^2 r_\zeta^2} r^2 \right], \end{aligned} \tag{38}$$

$$\psi(r) = -\frac{GM\eta_c}{3r} - \frac{G^2M^2}{2c^2r^2} \left[ \frac{2}{9}\eta_c^2 + \frac{3r_\eta - 2r_\zeta}{2r_\eta r_\zeta} r \right], \tag{39}$$

where  $\eta_c$  is set to 1 so as to recover GR in the limit of  $\phi(r)$ . The two length scales  $r_\eta$  and  $r_\zeta$  are the characteristic non-local parameters that define the scale at which the non-local gravity corrections become effective.

The first test of this form of the DW model has been carried out in [140], where the weak field non-local predictions have been compared against the NTT/VLT observations of

S2 star orbit [146]. Exploiting a modified Marquardt–Levenberg algorithm, the fit between the simulated orbit and the observed one has shown a slightly better agreement for the non-local model with respect to the Keplerian orbit. Moreover, some constraints have been set on the non-local length scales.

A further test has been subsequently performed in [141], exploiting the CLASH lensing data from 19 massive clusters [147,148]. The point-mass potentials of Equations (38) and (39) were extended to a spherically symmetric mass distribution, i.e., the Navarro–Frenk–White density profile, and the non-local predictions for the lensing convergence were achieved. Therefore, the MCMC analysis has highlighted two effective regimes in which the non-local model is able to match the observations at the same level of statistical significance as GR. In the high-value limit of the non-local parameters, the non-local model reduces to a GR-like theory, whose lensing strength is  $2/3$  of the standard one. In this scenario, the DW theory is thus able to fit the data at the cost of increased cluster mass estimates. On the other hand, approaching the low-value limit of the non-local length scales, the non-local corrections to the lensing potential become larger and comparable to the zeroth-order terms. In this regime, the non-local model is able to reproduce GR phenomenology, neither affecting the mass estimates nor the statistical viability of the model. Furthermore, when the non-local contributions becomes completely dominant, the non-local theory seems to be able to fit the lensing observations with extremely low cluster masses. Accordingly, an intriguing possibility to fit data with no dark matter emerges. Additional constraints on the non-local parameters were also derived.

The most recent astrophysical test of the exponential-DW model was carried out in [57], using the velocity distribution of elliptical galaxies [149]. Computing the non-local velocity dispersion as a function of the galaxy effective radius, the empirical relation of the so-called Fundamental Plane has been recovered so as to constrain the non-local gravity parameters. The results of the fit highlight the possibility to recover the fundamental plane without the dark matter hypothesis, setting new constraints for  $r_\eta$  and  $r_{\tilde{c}}$ .

It is worth noticing, however, that the non-local Deser–Woodard model exhibits worrisome features at the scale of the Solar System. Indeed, in [150], it was demonstrated that the screening mechanism proposed by the same authors of the non-local model does not work. As a consequence, the DW model would show a time dependence of the effective Newton constant in the small-scale limit, and it would be ruled out by Lunar Laser Ranging (LLR) observations. This conclusion, however, seems to be too strong, since it is still not clear how an FLRW background quantity behaves when evaluated from cosmological scales down to Solar System ones, where the system decouples from the Hubble flow. In fact, a full non-linear time- and scale-dependent solution around a non-linear structure would be necessary. A number of proposals go in this direction, and the so-called Vainshtein mechanism [151] can be regarded as the paradigm to realize the screening. Basically, any screening mechanism requires a scalar field coupled to matter and mediating a fifth force which might span from Solar System up to cosmological scales. Since non-local terms can be “localized”, thus resulting in effective scalar fields depending on the scale, some screening mechanism could naturally emerge so as to solve the above reported problems.

## 6.2. Testing the Ricci-Transverse Model by Solar System Observations and Gravitational Waves Detection

The main astrophysical tests of the RT model are related to Solar System observations. As we saw in the previous sub-section, any theory that extends GR has to reduce to Einstein’s theory at small scales. However, this is highly non-trivial when additional degrees of freedom are included, and screening mechanisms involving non-linear features are required. The RT model, instead, smoothly reduces to GR already at linear level, and no vDVZ discontinuity arises when  $m \rightarrow 0$  [56]. Note that such results are valid both in the flat and the Schwarzschild spacetime. Moreover, the non-local model passes the LLR test about the time variation of the effective Newton constant [150]. As stated in Equation (35),

indeed, the deviation parameter  $G_{eff}$  reduces to  $G_N$  as soon as the system’s characteristic scale decreases.

Another non-local feature of the RT model that has been investigated is the deviation from GR of the predicted gravitational radiation [152,153]. The RT model, similarly to some other extended theories of gravity such as  $f(R)$  gravity and DHOST theories, has survived the GW170817 event, which set a stringent constraint on the Gravitational Waves (GW) speed [154]. Indeed, this non-local model only modifies the friction term in the GW propagation equation, thus predicting a massless graviton. Moreover, neither the coupling with matter nor the gravitational interaction between the coalescing binaries are affected (the RT model reduces to GR at short distances), and the only difference will therefore be due to the free propagation of the GW from the source to the observer. The GW amplitude indeed undergoes a modified dampening in the non-local model

$$\tilde{h}_A(\eta, \mathbf{k}) \sim \frac{1}{d_L^{gw}(z)} = \left[ d_L^{em}(z) \exp \left\{ - \int_0^z \frac{dz'}{1+z'} \delta(z') \right\} \right]^{-1}, \tag{40}$$

where

$$\delta(\eta) = \frac{m^2 \bar{\mathcal{S}}_0(\eta)}{6H(\eta)}, \tag{41}$$

and  $\tilde{h}_A(\eta, \mathbf{k})$  are the Fourier modes of the GW amplitude, with  $A = \times, +$  labeling the polarization. Computing the ratio between the non-local behavior given by Equation (40) and the GR behavior,  $\tilde{h}_A(\eta, \mathbf{k}) \sim 1/d_L^{em}(z)$ , little deviation emerges for the RT-minimal model, while a 20 – 80% deviation manifests at large  $z$  for the RT formulations in which the auxiliary fields start their evolution during the de Sitter inflation. The more e-folds we consider between the onset of the auxiliary fields and the end of the inflation, the greater the deviation from GR. We can use a simple parametrization for the considered ratio

$$\frac{d_L^{gw}(z)}{d_L^{em}(z)} = \Xi_0 + \frac{1 - \Xi_0}{(1+z)^n}, \tag{42}$$

where  $\Xi_0$  is the asymptotic value reached by the ratio and  $n$  is the rate at which  $\Xi_0$  is approached. Then,

$$\delta(z) = \frac{\delta(0)}{1 - \Xi_0 + \Xi_0(1+z)^n}, \tag{43}$$

with  $\delta(0) = n(1 - \Xi_0)$ , and the event GW170817 provided the following constraint for such a parameter [153]:  $\delta(0) = -7.8_{-18.4}^{+9.7}$ . More stringent constraints will certainly be set with the next generation of GW detectors by exploiting the observations of GW events with electromagnetic counterparts.

### 7. Conclusions and Perspectives

In this paper, we reviewed the cosmological properties of two of the main proposals in the framework of the non-locally extended theories of gravity. In particular, we considered two metric IKGs that are inspired by quantum corrections and manifest a suitable cosmological behavior as well. Both the DW and RT models are able to reproduce the expansion history of the Universe, exhibiting a late-time accelerated expansion driven by the onset of the non-local corrections. The non-local extensions of the Hilbert–Einstein Lagrangian thus provide a viable mechanism to avoid the introduction of any form of unknown dark energy. Building on these appealing properties, we inquired into the chance of addressing the two main cosmological tensions, namely the  $\sigma_8$  and  $H_0$  tensions.

On the one hand, the non-local DW model has shown suitable features towards this aim. The phenomenological formulation of the model indeed predicts a lowered amplitude of growth of perturbations, therefore solving the  $\sigma_8$  tension. However, this model is made

equivalent to the  $\Lambda$ CDM cosmology at the background level, hence no chance to account for the Hubble tension arises. Another formulation of the DW theory, based on the Noether symmetries of the system, may address both the tensions. This model lacks a proper cosmological analysis, but the investigation of its lensing properties at the galaxy clusters scale has shown the same features that, in the phenomenological DW model, allow the weakening of the growth of structures. Moreover, this formulation of the non-local theory deviates from GR also at background level, thus enabling the possibility to alleviate the Hubble tension as well. The model has been also tested on astrophysical scales, and substantial statistical equivalence to GR has emerged in very different systems, such as the S2 star, the elliptical galaxies and the galaxy clusters. The main drawback of the DW model, however, is the absence of an effective screening mechanism on small scales, which has to be further investigated.

On the other hand, the non-local RT model perfectly reduces to GR at the Solar System scale, thus avoiding the necessity of non-trivial screening mechanisms. Accordingly, the model is not ruled out by the LLR test. Moreover, the non-minimal formulations of the RT model show a strong deviation from GR for what concerns the GW propagation at large redshift. A powerful tool to test the model with the next generation of GW detectors thus emerges. However, this non-local model is not able to address any of the cosmological tensions, as it mimics the  $\Lambda$ CDM evolution both at the background and linear perturbations level.

In view of the fact that the next generation of cosmological surveys are expected to provide sufficiently accurate data to reach a turning point in our comprehension of the Universe, it is of great interest to further investigate the main alternatives to GR. A complete cosmological analysis should especially be carried out for the non-local DW model in its formulation based on the Noether Symmetry Approach. This model indeed provides one of the most promising windows towards the solution of both the cosmological tensions and the dark energy problem. The large-scale structure especially appears as a privileged environment for testing the non-local models, since one of their main features is the emergence of characteristic length scales. However, it must be stressed that as long as no screening mechanism will be found for the DW model, its reliability will be compromised.

**Author Contributions:** Conceptualization, S.C.; Methodology, F.B. and V.S. All authors have read and agreed to the published version of the manuscript.

**Funding:** This research received no external funding.

**Data Availability Statement:** Public data in the literature were used.

**Acknowledgments:** This article is based upon work from COST Action CA21136 Addressing observational tensions in cosmology with systematic and fundamental physics (CosmoVerse) supported by COST (European Cooperation in Science and Technology). FB and SC acknowledge the support of *Istituto Nazionale di Fisica Nucleare (INFN), iniziative specifiche QGSKY and MOONLIGHT2*.

**Conflicts of Interest:** The authors declare no conflict of interest.

## Abbreviations

The following abbreviations are used in this manuscript:

BBN	Big Bang Nucleosynthesis
BAO	Baryon Acoustic Oscillations
$\Lambda$ CDM	Lambda Cold Dark Matter
GR	General Relativity
DE	Dark Energy
DM	Dark Matter
CMB	Cosmic Microwave Background

WL	Weak Lensing
CC	Cluster Counts
RSD	Redshift Space Distortion
DW	Deser–Woodard
RT	Ricci-Transverse
QFT	Quantum Field Theory
IDG	Infinite Derivative Theory of Gravity
IKG	Integral Kernel Theory of Gravity
UV	UltraViolet
IR	InfraRed
SNIa	Type Ia Supernovae
FLRW	Friedmann–Lemaître–Robertson–Walker
MCMC	Markov Chain Monte Carlo
LLR	Lunar Laser Ranging
GW	Gravitational Waves

## Notes

$$^1 \quad \mathcal{E}^{\mu\nu,\alpha\beta} = \frac{1}{2}(\eta^{\mu\rho}\eta^{\nu\sigma} + \eta^{\mu\sigma}\eta^{\nu\rho} - 2\eta^{\mu\nu}\eta^{\rho\sigma})\square + (\eta^{\rho\sigma}\partial^\mu\partial^\nu + \eta^{\mu\nu}\partial^\rho\partial^\sigma) - \frac{1}{2}(\eta^{\mu\rho}\partial^\sigma\partial^\nu + \eta^{\nu\rho}\partial^\sigma\partial^\mu + \eta^{\mu\sigma}\partial^\rho\partial^\nu + \eta^{\mu\sigma}\partial^\rho\partial^\mu)$$

## References

- Hogg, D.W.; Eisenstein, D.J.; Blanton, M.R.; Bahcall, N.A.; Brinkmann, J.; Gunn, J.E.; Schneider, D.P. Cosmic homogeneity demonstrated with luminous red galaxies. *Astrophys. J.* **2005**, *624*, 54.
- Labini, F.S.; Vasilyev, N.L.; Pietronero, L.; Baryshev, Y.V. Absence of self-averaging and of homogeneity in the large-scale galaxy distribution. *Europhys. Lett.* **2009**, *86*, 49001. [[CrossRef](#)]
- Riess, A.G.; Filippenko, A.V.; Challis, P.; Clocchiatti, A.; Diercks, A.; Garnavich, P.M.; Gilliland, R.L.; Hogan, C.J.; Jha, S.; Kirshner, R.P.; et al. Observational Evidence from Supernovae for an Accelerating Universe and a Cosmological Constant. *Astron. J.* **1998**, *116*, 1009. [[CrossRef](#)]
- Perlmutter, S.; Aldering, G.; Goldhaber, G.; Knop, R.A.; Nugent, P.; Castro, P.G.; Deustua, S.; Fabbro, S.; Goobar, A.; Groom, D.E.; et al. Measurements of  $\Omega$  and  $\Lambda$  from 42 High-Redshift Supernovae. *Astrophys. J.* **1999**, *517*, 565. [[CrossRef](#)]
- Aghanim, N.; Akrami, Y.; Ashdown, M.; Aumont, J.; Baccigalupi, C.; Ballardini, M.; Banday, A.J.; Barreiro, R.B.; Bartolo, N.; Basak, S.; et al. Planck 2018 results. VI. Cosmological parameters. *Astron. Astrophys.* **2020**, *641*, A6; Erratum in *Astron. Astrophys.* **2021**, *652*, C4.
- Alam, S.; Aubert, M.; Avila, S.; Balland, C.; Bautista, J.E.; Bershad, M.A.; Bizyaev, D.; Blanton, M.R.; Bolton, A.S.; Bovy, J.; et al. Completed SDSS-IV extended Baryon Oscillation Spectroscopic Survey: Cosmological implications from two decades of spectroscopic surveys at the Apache Point Observatory. *Phys. Rev. D* **2021**, *103*, 083533. [[CrossRef](#)]
- Abbott, T.; Aguena, M.; Alarcon, A.; Allam, S.; Alves, O.; Amon, A.; Andrade-Oliveira, F.; Annis, J.; Avila, S.; Bacon, D.; et al. Dark Energy Survey Year 3 results: Cosmological constraints from galaxy clustering and weak lensing. *Phys. Rev. D* **2022**, *105*, 023520. [[CrossRef](#)]
- Bull, P.; Akrami, Y.; Adamek, J.; Baker, T.; Bellini, E.; Jiménez, J.B.; Bentivegna, E.; Camera, S.; Clesse, S.; Davis, J.H.; et al. Beyond  $\Lambda$ CDM: Problems, solutions, and the road ahead. *Phys. Dark Universe* **2016**, *12*, 56–99. [[CrossRef](#)]
- Perivolaropoulos, L.; Skara, F. Challenges for  $\Lambda$ CDM: An update. *New Astron. Rev.* **2022**, *95*, 101659. [[CrossRef](#)]
- Di Valentino, E.; Anchordoqui, L.A.; Özgür Akarsu.; Ali-Haimoud, Y.; Amendola, L.; Arendse, N.; Asgari, M.; Ballardini, M.; Basilakos, S.; Battistelli, E.; et al. Snowmass2021—Letter of interest cosmology intertwined II: The hubble constant tension. *Astropart. Phys.* **2021**, *131*, 102605. [[CrossRef](#)]
- Di Valentino, E.; Anchordoqui, L.A.; Özgür Akarsu.; Ali-Haimoud, Y.; Amendola, L.; Arendse, N.; Asgari, M.; Ballardini, M.; Basilakos, S.; Battistelli, E.; et al. Cosmology intertwined III:  $f\sigma_8$  and  $S_8$ . *Astropart. Phys.* **2021**, *131*, 102604. [[CrossRef](#)]
- Bertone, G.; Hooper, D.; Silk, J. Particle dark matter: Evidence, candidates and constraints. *Phys. Rep.* **2005**, *405*, 279–390. [[CrossRef](#)]
- Batista, R.A.; Amin, M.A.; Barenboim, G.; Bartolo, N.; Baumann, D.; Bauswein, A.; Bellini, E.; Benisty, D.; Bertone, G.; Blasi, P.; et al. EuCAPT White Paper: Opportunities and Challenges for Theoretical Astroparticle Physics in the Next Decade. *arXiv* **2021**, arXiv:2110.10074. [[CrossRef](#)]
- Copeland, E.J.; Sami, M.; Tsujikawa, S. Dynamics of dark energy. *Int. J. Mod. Phys. D* **2006**, *15*, 1753–1935.
- Padmanabhan, T. Cosmological constant: The Weight of the vacuum. *Phys. Rept.* **2003**, *380*, 235–320.
- Nojiri, S.; Odintsov, S.D. Introduction to modified gravity and gravitational alternative for dark energy. *Int. J. Geom. Methods Mod. Phys.* **2007**, *4*, 115–145. [[CrossRef](#)]
- Riess, A.G.; Yuan, W.; Macri, L.M.; Scolnic, D.; Brout, D.; Casertano, S.; Jones, D.O.; Murakami, Y.; Anand, G.S.; Breuval, L.; et al. A Comprehensive Measurement of the Local Value of the Hubble Constant with 1 km s<sup>-1</sup> Mpc<sup>-1</sup> Uncertainty from the Hubble Space Telescope and the SH0ES Team. *Astrophys. J. Lett.* **2022**, *934*, L7. [[CrossRef](#)]

18. Asgari, M.; Lin, C.A.; Joachimi, B.; Giblin, B.; Heymans, C.; Hildebrandt, H.; Kannawadi, A.; Stözlner, B.; Tröster, T.; van den Busch, J.L.; et al. KiDS-1000 cosmology: Cosmic shear constraints and comparison between two point statistics. *Astron. Astrophys.* **2021**, *645*, A104. [[CrossRef](#)]
19. Lesci, G.F.; Marulli, F.; Moscardini, L.; Sereno, M.; Veropalumbo, A.; Maturi, M.; Giocoli, C.; Radovich, M.; Bellagamba, F.; Roncarelli, M.; et al. AMICO galaxy clusters in KiDS-DR3: Cosmological constraints from counts and stacked weak lensing. *Astron. Astrophys.* **2022**, *659*, A88. [[CrossRef](#)]
20. Chen, S.F.; Vlah, Z.; White, M. A new analysis of galaxy 2-point functions in the BOSS survey, including full-shape information and post-reconstruction BAO. *J. Cosmol. Astropart. Phys.* **2022**, *2022*, 8. [[CrossRef](#)]
21. Capozziello, S. Curvature Quintessence. *Int. J. Mod. Phys. D* **2002**, *11*, 483–491. [[CrossRef](#)]
22. Nojiri, S.; Odintsov, S.D. Modified  $f(R)$  gravity consistent with realistic cosmology: From a matter dominated epoch to a dark energy universe. *Phys. Rev. D* **2006**, *74*, 086005. [[CrossRef](#)]
23. Starobinsky, A.A. Disappearing cosmological constant in  $f(R)$  gravity. *JETP Lett.* **2007**, *86*, 157–163. [[CrossRef](#)]
24. Fay, S.; Nesseris, S.; Perivolaropoulos, L. Can  $f(R)$  Modified Gravity Theories Mimic a  $\Lambda$ CDM Cosmology? *Phys. Rev. D* **2007**, *76*, 063504.
25. Lazkoz, R.; Ortiz-Baños, M.; Salzano, V.  $f(R)$  gravity modifications: From the action to the data. *Eur. Phys. J. C* **2018**, *78*, 213. [[CrossRef](#)] [[PubMed](#)]
26. Bajardi, F.; D’Agostino, R.; Benetti, M.; De Falco, V.; Capozziello, S. Early and late time cosmology: The  $f(R)$  gravity perspective. *Eur. Phys. J. Plus* **2022**, *137*, 1239. [[CrossRef](#)]
27. D’Agostino, R.; Nunes, R.C. Measurements of  $H_0$  in modified gravity theories: The role of lensed quasars in the late-time Universe. *Phys. Rev. D* **2020**, *101*, 103505. [[CrossRef](#)]
28. Nesseris, S.; Basilakos, S.; Saridakis, E.N.; Perivolaropoulos, L. Viable  $f(T)$  models are practically indistinguishable from  $\Lambda$ CDM. *Phys. Rev. D* **2013**, *88*, 103010.
29. Cai, Y.F.; Capozziello, S.; De Laurentis, M.; Saridakis, E.N.  $f(T)$  teleparallel gravity and cosmology. *Rep. Prog. Phys.* **2016**, *79*, 106901. [[CrossRef](#)]
30. Golovnev, A.; Koivisto, T. Cosmological perturbations in modified teleparallel gravity models. *J. Cosmol. Astropart. Phys.* **2018**, *11*, 12.
31. Wang, D.; Mota, D. Can  $f(T)$  gravity resolve the  $H_0$  tension? *Phys. Rev. D* **2020**, *102*, 063530. [[CrossRef](#)]
32. Bahamonde, S.; Dialektopoulos, K.F.; Escamilla-Rivera, C.; Farrugia, G.; Gakis, V.; Hendry, M.; Hohmann, M.; Said, J.L.; Mifsud, J.; Di Valentino, E. Teleparallel Gravity: From Theory to Cosmology. *Rep. Prog. Phys.* **2022**. [[CrossRef](#)] [[PubMed](#)]
33. Nojiri, S.; Odintsov, S.D. Modified Gauss-Bonnet theory as gravitational alternative for dark energy. *Phys. Lett. B* **2005**, *631*, 1–6.
34. Li, B.; Barrow, J.D.; Mota, D.F. The Cosmology of Modified Gauss-Bonnet Gravity. *Phys. Rev. D* **2007**, *76*, 044027.
35. Myrzakulov, R.; Saez-Gomez, D.; Tureanu, A. On the  $\Lambda$ CDM Universe in  $f(G)$  gravity. *Gen. Relativ. Gravit.* **2011**, *43*, 1671–1684.
36. Bajardi, F.; Capozziello, S.  $f(\mathcal{G})$  Noether cosmology. *Eur. Phys. J. C* **2020**, *80*, 704. [[CrossRef](#)]
37. Capozziello, S.; Nesseris, S.; Perivolaropoulos, L. Reconstruction of the Scalar-Tensor Lagrangian from a  $\Lambda$ CDM Background and Noether Symmetry. *J. Cosmol. Astropart. Phys.* **2007**, *12*, 009.
38. Heisenberg, L. A systematic approach to generalisations of General Relativity and their cosmological implications. *Phys. Rept.* **2019**, *796*, 1–113.
39. Langlois, D. Dark energy and modified gravity in degenerate higher-order scalar-tensor (DHOST) theories: A review. *Int. J. Mod. Phys. D* **2019**, *28*, 1942006.
40. D’Agostino, R.; Luongo, O. Growth of matter perturbations in nonminimal teleparallel dark energy. *Phys. Rev. D* **2018**, *98*, 124013. [[CrossRef](#)]
41. Bajardi, F.; Capozziello, S. Equivalence of nonminimally coupled cosmologies by Noether symmetries. *Int. J. Mod. Phys. D* **2020**, *29*, 2030015. [[CrossRef](#)]
42. Amendola, L.; Campos, G.C.; Rosenfeld, R. Consequences of dark matter-dark energy interaction on cosmological parameters derived from type Ia supernova data. *Phys. Rev. D* **2007**, *75*, 083506. [[CrossRef](#)]
43. Wang, B.; Abdalla, E.; Atrio-Barandela, F.; Pavón, D. Dark matter and dark energy interactions: Theoretical challenges, cosmological implications and observational signatures. *Rep. Prog. Phys.* **2016**, *79*, 096901. [[CrossRef](#)] [[PubMed](#)]
44. Di Valentino, E.; Melchiorri, A.; Mena, O. Can interacting dark energy solve the  $H_0$  tension? *Phys. Rev. D* **2017**, *96*, 043503. [[CrossRef](#)]
45. Asghari, M.; Jiménez, J.B.; Khosravi, S.; Mota, D.F. On structure formation from a small-scales-interacting dark sector. *J. Cosmol. Astropart. Phys.* **2019**, *2019*, 042. [[CrossRef](#)]
46. Yang, W.; Vagnozzi, S.; Di Valentino, E.; Nunes, R.C.; Pan, S.; Mota, D.F. Listening to the sound of dark sector interactions with gravitational wave standard sirens. *J. Cosmol. Astropart. Phys.* **2019**, *2019*, 037. [[CrossRef](#)]
47. Saridakis, E.N.; Lazkoz, R.; Salzano, V.; Moniz, P.V.; Capozziello, S.; Jiménez, J.B.; De Laurentis, M.; Olmo, G.J. Modified Gravity and Cosmology: An Update by the CANTATA Network; Springer: Cham, Switzerland, 2021.
48. Di Valentino, E.; Mena, O.; Pan, S.; Visinelli, L.; Yang, W.; Melchiorri, A.; Mota, D.F.; Riess, A.G.; Silk, J. In the realm of the Hubble tension—A review of solutions. *Class. Quant. Grav.* **2021**, *38*, 153001.
49. Capozziello, S.; Bajardi, F. Nonlocal gravity cosmology: An overview. *Int. J. Mod. Phys. D* **2021**, *31*, 2230009. [[CrossRef](#)]
50. Deser, S.; Woodard, R.P. Nonlocal Cosmology. *Phys. Rev. Lett.* **2007**, *99*, 111301. [[CrossRef](#)]
51. Maggiore, M. Phantom dark energy from nonlocal infrared modifications of general relativity. *Phys. Rev. D* **2014**, *89*, 043008. [[CrossRef](#)]

52. Buoninfante, L. Nonlocal Field Theories: Theoretical and Phenomenological Aspects. Ph.D. Thesis, University of Groningen, Groningen, The Netherlands, 2019. [\[CrossRef\]](#)
53. Biswas, T.; Gerwick, E.; Koivisto, T.; Mazumdar, A. Towards Singularity- and Ghost-Free Theories of Gravity. *Phys. Rev. Lett.* **2012**, *108*, 031101. [\[CrossRef\]](#) [\[PubMed\]](#)
54. Briscese, F.; Marcianò, A.; Modesto, L.; Saridakis, E.N. Inflation in (super-)renormalizable gravity. *Phys. Rev. D* **2013**, *87*, 083507. [\[CrossRef\]](#)
55. Biswas, T.; Mazumdar, A.; Siegel, W. Bouncing universes in string-inspired gravity. *J. Cosmol. Astropart. Phys.* **2006**, *2006*, 009. [\[CrossRef\]](#)
56. Belgacem, E.; Dirian, Y.; Finke, A.; Foffa, S.; Maggiore, M. Gravity in the infrared and effective nonlocal models. *J. Cosmol. Astropart. Phys.* **2020**, *2020*, 010. [\[CrossRef\]](#)
57. Borka, D.; Borka Jovanović, V.; Capozziello, S.; Jovanović, P. Velocity distribution of elliptical galaxies in the framework of Non-local Gravity model. *Adv. Space Res.* **2022**, *in press*. [\[CrossRef\]](#)
58. Strominger, A. *Lectures on the Infrared Structure of Gravity and Gauge Theory*; Princeton University Press: Princeton, NJ, USA, 2018. [\[CrossRef\]](#)
59. Reuter, M.; Saueressig, F. A class of nonlocal truncations in quantum Einstein gravity and its renormalization group behavior. *Phys. Rev. D* **2002**, *66*, 125001. [\[CrossRef\]](#)
60. Wetterich, C. Infrared limit of quantum gravity. *Phys. Rev. D* **2018**, *98*, 026028. [\[CrossRef\]](#)
61. Barvinsky, A.O.; Gusev, Y.V.; Mukhanov, V.F.; Nesterov, D.V. Nonperturbative late time asymptotics for heat kernel in gravity theory. *Phys. Rev. D* **2003**, *68*, 105003.
62. Barvinsky, A.O. Aspects of nonlocality in quantum field theory, quantum gravity and cosmology. *Mod. Phys. Lett. A* **2015**, *30*, 1540003. [\[CrossRef\]](#)
63. Maggiore, M. Nonlocal Infrared Modifications of Gravity. A Review. In *Gravity and the Quantum*; Springer: Cham, Switzerland, 2017; pp. 221–281. [\[CrossRef\]](#)
64. Nojiri, S.; Odintsov, S.D. Modified non-local- $F(R)$  gravity as the key for the inflation and dark energy. *Phys. Lett. B* **2008**, *659*, 821–826. [\[CrossRef\]](#)
65. Kehagias, A.; Maggiore, M. Spherically symmetric static solutions in a nonlocal infrared modification of General Relativity. *J. High Energy Phys.* **2014**, *2014*, 29. [\[CrossRef\]](#)
66. Aiola, S.; Calabrese, E.; Maurin, L.; Naess, S.; Schmitt, B.L.; Abitbol, M.H.; Addison, G.E.; Ade, P.A.R.; Alonso, D.; Amiri, M.; et al. The Atacama Cosmology Telescope: DR4 maps and cosmological parameters. *J. Cosmol. Astropart. Phys.* **2020**, *2020*, 47. [\[CrossRef\]](#)
67. Tröster, T.; Asgari, M.; Blake, C.; Cataneo, M.; Heymans, C.; Hildebrandt, H.; Joachimi, B.; Lin, C.A.; Sánchez, A.G.; Wright, A.H.; et al. KiDS-1000 Cosmology: Constraints beyond flat  $\Lambda$ CDM. *Astron. Astrophys.* **2021**, *649*, A88. [\[CrossRef\]](#)
68. Pandey, S.; Krause, E.; DeRose, J.; MacCrann, N.; Jain, B.; Crocce, M.; Blazek, J.; Choi, A.; Huang, H.; To, C.; et al. Dark Energy Survey year 3 results: Constraints on cosmological parameters and galaxy-bias models from galaxy clustering and galaxy-galaxy lensing using the redMaGiC sample. *Phys. Rev. D* **2022**, *106*, 043520. [\[CrossRef\]](#)
69. Weinberg, S. The cosmological constant problem. *Rev. Mod. Phys.* **1989**, *61*, 1. [\[CrossRef\]](#)
70. Velten, H.E.S.; vom Marttens, R.F.; Zimdahl, W. Aspects of the cosmological “coincidence problem”. *Eur. Phys. J. C* **2014**, *74*, 3160. [\[CrossRef\]](#)
71. Deffayet, C.; Woodard, R. Reconstructing the distortion function for nonlocal cosmology. *J. Cosmol. Astropart. Phys.* **2009**, *2009*, 23. [\[CrossRef\]](#)
72. Foffa, S.; Maggiore, M.; Mitsou, E. Cosmological dynamics and dark energy from nonlocal infrared modifications of gravity. *Int. J. Mod. Phys. A* **2014**, *29*, 1450116. [\[CrossRef\]](#)
73. Calabrese, E.; Slosar, A.; Melchiorri, A.; Smoot, G.F.; Zahn, O. Cosmic microwave weak lensing data as a test for the dark universe. *Phys. Rev. D* **2008**, *77*, 123531. [\[CrossRef\]](#)
74. Hildebrandt, H.; Viola, M.; Heymans, C.; Joudaki, S.; Kuijken, K.; Blake, C.; Erben, T.; Joachimi, B.; Klaes, D.; Miller, L.; et al. KiDS-450: Cosmological parameter constraints from tomographic weak gravitational lensing. *Mon. Not. R. Astron. Soc.* **2016**, *465*, 1454–1498. [\[CrossRef\]](#)
75. Hildebrandt, H.; Köhlinger, F.; van den Busch, J.L.; Joachimi, B.; Heymans, C.; Kannawadi, A.; Wright, A.H.; Asgari, M.; Blake, C.; Hoekstra, H.; et al. KiDS+VIKING-450: Cosmic shear tomography with optical and infrared data. *Astron. Astrophys.* **2020**, *633*, A69. [\[CrossRef\]](#)
76. Köhlinger, F.; Viola, M.; Joachimi, B.; Hoekstra, H.; van Uitert, E.; Hildebrandt, H.; Choi, A.; Erben, T.; Heymans, C.; Joudaki, S.; et al. KiDS-450: The tomographic weak lensing power spectrum and constraints on cosmological parameters. *Mon. Not. R. Astron. Soc.* **2017**, *471*, 4412–4435. [\[CrossRef\]](#)
77. Wright, A.H.; Hildebrandt, H.; van den Busch, J.L.; Heymans, C.; Joachimi, B.; Kannawadi, A.; Kuijken, K. KiDS+VIKING-450: Improved cosmological parameter constraints from redshift calibration with self-organising maps. *Astron. Astrophys.* **2020**, *640*, L14. [\[CrossRef\]](#)
78. Troxel, M.; MacCrann, N.; Zuntz, J.; Eifler, T.; Krause, E.; Dodelson, S.; Gruen, D.; Blazek, J.; Friedrich, O.; Samuroff, S.; et al. Dark Energy Survey Year 1 results: Cosmological constraints from cosmic shear. *Phys. Rev. D* **2018**, *98*, 043528. [\[CrossRef\]](#)
79. Joudaki, S.; Hildebrandt, H.; Traykova, D.; Chisari, N.E.; Heymans, C.; Kannawadi, A.; Kuijken, K.; Wright, A.H.; Asgari, M.; Erben, T.; et al. KiDS+VIKING-450 and DES-Y1 combined: Cosmology with cosmic shear. *Astron. Astrophys.* **2020**, *638*, L1. [\[CrossRef\]](#)

80. Asgari, M.; Tröster, T.; Heymans, C.; Hildebrandt, H.; van den Busch, J.L.; Wright, A.H.; Choi, A.; Erben, T.; Joachimi, B.; Joudaki, S.; et al. KiDS+VIKING-450 and DES-Y1 combined: Mitigating baryon feedback uncertainty with COSEBIs. *Astron. Astrophys.* **2020**, *634*, A127. [[CrossRef](#)]
81. Loureiro, A.; Whittaker, L.; Mancini, A.S.; Joachimi, B.; Cuceu, A.; Asgari, M.; Stözlner, B.; Tröster, T.; Wright, A.H.; Bilicki, M.; et al. KiDS and Euclid: Cosmological implications of a pseudo angular power spectrum analysis of KiDS-1000 cosmic shear tomography. *Astron. Astrophys.* **2022**, *665*. [[CrossRef](#)]
82. Chang, C.; Omori, Y.; Baxter, E.J.; Doux, C.; Choi, A.; Pandey, S.; Alarcon, A.; Alves, O.; Amon, A.; Andrade-Oliveira, F.; et al. Joint analysis of DES Year 3 data and CMB lensing from SPT and Planck II: Cross-correlation measurements and cosmological constraints. *arXiv* **2022**, arXiv:2203.12440. [[CrossRef](#)]
83. Amon, A.; Gruen, D.; Troxel, M.; MacCrann, N.; Dodelson, S.; Choi, A.; Doux, C.; Secco, L.; Samuroff, S.; Krause, E.; et al. Dark Energy Survey Year 3 results: Cosmology from cosmic shear and robustness to data calibration. *Phys. Rev. D* **2022**, *105*, 023514. [[CrossRef](#)]
84. Secco, L.; Samuroff, S.; Krause, E.; Jain, B.; Blazek, J.; Raveri, M.; Campos, A.; Amon, A.; Chen, A.; Doux, C.; et al. Dark Energy Survey Year 3 results: Cosmology from cosmic shear and robustness to modeling uncertainty. *Phys. Rev. D* **2022**, *105*, 023515. [[CrossRef](#)]
85. Heymans, C.; Tröster, T.; Asgari, M.; Blake, C.; Hildebrandt, H.; Joachimi, B.; Kuijken, K.; Lin, C.A.; Sánchez, A.G.; van den Busch, J.L.; et al. KiDS-1000 Cosmology: Multi-probe weak gravitational lensing and spectroscopic galaxy clustering constraints. *Astron. Astrophys.* **2021**, *646*, A140. [[CrossRef](#)]
86. Mantz, A.B.; von der Linden, A.; Allen, S.W.; Applegate, D.E.; Kelly, P.L.; Morris, R.G.; Rapetti, D.A.; Schmidt, R.W.; Adhikari, S.; Allen, M.T.; et al. Weighing the giants – IV. Cosmology and neutrino mass. *Mon. Not. R. Astron. Soc.* **2014**, *446*, 2205–2225. [[CrossRef](#)]
87. Salvati, L.; Douspis, M.; Aghanim, N. Constraints from thermal Sunyaev-Zel’dovich cluster counts and power spectrum combined with CMB. *Astron. Astrophys.* **2018**, *614*, A13. [[CrossRef](#)]
88. Costanzi, M.; Rozo, E.; Simet, M.; Zhang, Y.; Evrard, A.E.; Mantz, A.; Rykoff, E.S.; Jeltema, T.; Gruen, D.; Allen, S.; et al. Methods for cluster cosmology and application to the SDSS in preparation for DES Year 1 release. *Mon. Not. R. Astron. Soc.* **2019**, *488*, 4779–4800. [[CrossRef](#)]
89. Bocquet, S.; Dietrich, J.P.; Schrabback, T.; Bleem, L.E.; Klein, M.; Allen, S.W.; Applegate, D.E.; Ashby, M.L.N.; Bautz, M.; Bayliss, M.; et al. Cluster Cosmology Constraints from the 2500 deg<sup>2</sup> SPT-SZ Survey: Inclusion of Weak Gravitational Lensing Data from Magellan and the Hubble Space Telescope. *Astrophys. J.* **2019**, *878*, 55. [[CrossRef](#)]
90. Abbott, T.; Aguena, M.; Alarcon, A.; Allam, S.; Allen, S.; Annis, J.; Avila, S.; Bacon, D.; Bechtol, K.; Bermeo, A.; et al. Dark Energy Survey Year 1 Results: Cosmological constraints from cluster abundances and weak lensing. *Phys. Rev. D* **2020**, *102*, 023509. [[CrossRef](#)]
91. Abdullah, M.H.; Klypin, A.; Wilson, G. Cosmological Constraints on  $\Omega_M$  and  $\sigma_8$  from Cluster Abundances Using the GalWCat19 Optical-spectroscopic SDSS Catalog. *Astrophys. J.* **2020**, *901*, 90. [[CrossRef](#)]
92. Kazantzidis, L.; Perivolaropoulos, L. Evolution of the  $f\sigma_8$  tension with the Planck15/ $\Lambda$ CDM determination and implications for modified gravity theories. *Phys. Rev. D* **2018**, *97*, 103503. [[CrossRef](#)]
93. Benisty, D. Quantifying the  $S_8$  tension with the Redshift Space Distortion data set. *Phys. Dark Universe* **2021**, *31*, 100766. [[CrossRef](#)]
94. Nunes, R.C.; Vagnozzi, S. Arbitrating the  $S_8$  discrepancy with growth rate measurements from redshift-space distortions. *Mon. Not. R. Astron. Soc.* **2021**, *505*, 5427–5437. [[CrossRef](#)]
95. Philcox, O.H.; Ivanov, M.M. BOSS DR12 full-shape cosmology:  $\Lambda$ CDM constraints from the large-scale galaxy power spectrum and bispectrum monopole. *Phys. Rev. D* **2022**, *105*, 043517. [[CrossRef](#)]
96. Nersisyan, H.; Cid, A.F.; Amendola, L. Structure formation in the Deser-Woodard nonlocal gravity model: A reappraisal. *J. Cosmol. Astropart. Phys.* **2017**, *2017*, 46. [[CrossRef](#)]
97. Park, S. Revival of the Deser-Woodard nonlocal gravity model: Comparison of the original nonlocal form and a localized formulation. *Phys. Rev. D* **2018**, *97*, 044006. [[CrossRef](#)]
98. Amendola, L.; Dirian, Y.; Nersisyan, H.; Park, S. Observational constraints in nonlocal gravity: The Deser-Woodard case. *J. Cosmol. Astropart. Phys.* **2019**, *2019*, 45. [[CrossRef](#)]
99. Joudaki, S.; Blake, C.; Heymans, C.; Choi, A.; Harnois-Deraps, J.; Hildebrandt, H.; Joachimi, B.; Johnson, A.; Mead, A.; Parkinson, D.; et al. CFHTLenS revisited: Assessing concordance with Planck including astrophysical systematics. *Mon. Not. R. Astron. Soc.* **2016**, *465*, 2033–2052. [[CrossRef](#)]
100. Ivanov, M.M. Cosmological constraints from the power spectrum of eBOSS emission line galaxies. *Phys. Rev. D* **2021**, *104*, 103514. [[CrossRef](#)]
101. Ivanov, M.M.; Simonović, M.; Zaldarriaga, M. Cosmological parameters from the BOSS galaxy power spectrum. *J. Cosmol. Astropart. Phys.* **2020**, *2020*, 42. [[CrossRef](#)]
102. White, M.; Zhou, R.; DeRose, J.; Ferraro, S.; Chen, S.F.; Kokron, N.; Bailey, S.; Brooks, D.; García-Bellido, J.; Guy, J.; et al. Cosmological constraints from the tomographic cross-correlation of DESI Luminous Red Galaxies and Planck CMB lensing. *J. Cosmol. Astropart. Phys.* **2022**, *2022*, 7. [[CrossRef](#)]
103. Jeffreys, H. *The Theory of Probability*; Oxford University Press: Oxford, UK, 1998.
104. Nesseris, S.; Tsujikawa, S. Cosmological perturbations and observational constraints on nonlocal massive gravity. *Phys. Rev. D* **2014**, *90*, 024070. [[CrossRef](#)]

105. Dutcher, D.; Balkenhol, L.; Ade, P.; Ahmed, Z.; Anderes, E.; Anderson, A.; Archibley, M.; Avva, J.; Aylor, K.; Barry, P.; et al. Measurements of the E-mode polarization and temperature-E-mode correlation of the CMB from SPT-3G 2018 data. *Phys. Rev. D* **2021**, *104*, 022003. [[CrossRef](#)]
106. Wang, K.; Huang, Q.G. Implications for cosmology from ground-based Cosmic Microwave Background observations. *J. Cosmol. Astropart. Phys.* **2020**, *2020*, 045. [[CrossRef](#)]
107. Balkenhol, L.; Dutcher, D.; Ade, P.; Ahmed, Z.; Anderes, E.; Anderson, A.; Archibley, M.; Avva, J.; Aylor, K.; Barry, P.; et al. Constraints on  $\Lambda$ CDM extensions from the SPT-3G 2018 EE and TE power spectra. *Phys. Rev. D* **2021**, *104*, 083509. [[CrossRef](#)]
108. Addison, G.E. High  $H_0$  values from CMB E-mode Data: A Clue for Resolving the Hubble Tension? *Astrophys. J. Lett.* **2021**, *912*, L1. [[CrossRef](#)]
109. D'Amico, G.; Gleyzes, J.; Kokron, N.; Markovic, K.; Senatore, L.; Zhang, P.; Beutler, F.; Gil-Marín, H. The cosmological analysis of the SDSS/BOSS data from the Effective Field Theory of Large-Scale Structure. *J. Cosmol. Astropart. Phys.* **2020**, *2020*, 5. [[CrossRef](#)]
110. Colas, T.; d'Amico, G.; Senatore, L.; Zhang, P.; Beutler, F. Efficient cosmological analysis of the SDSS/BOSS data from the Effective Field Theory of Large-Scale Structure. *J. Cosmol. Astropart. Phys.* **2020**, *2020*, 1. [[CrossRef](#)]
111. Cooke, R.J.; Pettini, M.; Steidel, C.C. One Percent Determination of the Primordial Deuterium Abundance. *Astrophys. J.* **2018**, *855*, 102. [[CrossRef](#)]
112. Scolnic, D.M.; Jones, D.O.; Rest, A.; Pan, Y.C.; Chornock, R.; Foley, R.J.; Huber, M.E.; Kessler, R.; Narayan, G.; Riess, A.G.; et al. The Complete Light-curve Sample of Spectroscopically Confirmed SNe Ia from Pan-STARRS1 and Cosmological Constraints from the Combined Pantheon Sample. *Astrophys. J.* **2018**, *859*, 101. [[CrossRef](#)]
113. Abbott, T.; Abdalla, F.; Alarcon, A.; Aleksic, J.; Allam, S.; Allen, S.; Amara, A.; Annis, J.; Asorey, J.; Avila, S.; et al. Dark Energy Survey year 1 results: Cosmological constraints from galaxy clustering and weak lensing. *Phys. Rev. D* **2018**, *98*, 043526. [[CrossRef](#)]
114. Krause, E.; Eifler, T.F.; Zuntz, J.; Friedrich, O.; Troxel, M.A.; Dodelson, S.; Blazek, J.; Secco, L.F.; MacCrann, N.; Baxter, E.; et al. Dark Energy Survey Year 1 Results: Multi-Probe Methodology and Simulated Likelihood Analyses. *arXiv* **2017**, arXiv:1706.09359. [[CrossRef](#)]
115. Riess, A.G. The expansion of the Universe is faster than expected. *Nat. Rev. Phys.* **2019**, *2*, 10–12. [[CrossRef](#)]
116. Riess, A.G.; Macri, L.; Casertano, S.; Lampeitl, H.; Ferguson, H.C.; Filippenko, A.V.; Jha, S.W.; Li, W.; Chornock, R. A 3% solution: Determination of the Hubble constant with the Hubble Space Telescope and the Wide Field Camera 3. *Astrophys. J.* **2011**, *730*, 119. [[CrossRef](#)]
117. Riess, A.G.; Macri, L.M.; Hoffmann, S.L.; Scolnic, D.; Casertano, S.; Filippenko, A.V.; Tucker, B.E.; Reid, M.J.; Jones, D.O.; Silverman, J.M.; et al. A 2.4% determination of the local value of the Hubble constant. *Astrophys. J.* **2016**, *826*, 56. [[CrossRef](#)]
118. Riess, A.G.; Casertano, S.; Yuan, W.; Bowers, J.B.; Macri, L.; Zinn, J.C.; Scolnic, D. Cosmic Distances Calibrated to 1% Precision with Gaia EDR3 Parallaxes and Hubble Space Telescope Photometry of 75 Milky Way Cepheids Confirm Tension with  $\Lambda$ CDM. *Astrophys. J. Lett.* **2021**, *908*, L6. [[CrossRef](#)]
119. Gaia Collaboration.; Brown, A.G.A.; Vallenari, A.; Prusti, T.; de Bruijne, J.H.J.; Babusiaux, C.; Biermann, M.; Creevey, O.L.; Evans, D.W.; Eyer, L.; et al. Gaia Early Data Release 3—Summary of the contents and survey properties. *Astron. Astrophys.* **2021**, *649*. [[CrossRef](#)]
120. Lindegren, L.; Bastian, U.; Biermann, M.; Bombrun, A.; de Torres, A.; Gerlach, E.; Geyer, R.; Hernández, J.; Hilger, T.; Hobbs, D.; et al. Gaia Early Data Release 3 - Parallax bias versus magnitude, colour, and position. *Astronomy & Astrophysics* **2021**, *649*, A1. [[CrossRef](#)]
121. Wong, K.C.; Suyu, S.H.; Chen, G.C.F.; Rusu, C.E.; Millon, M.; Sluse, D.; Bonvin, V.; Fassnacht, C.D.; Taubenberger, S.; Auger, M.W.; et al. H0LiCOW - XIII. A 2.4 per cent measurement of  $H_0$  from lensed quasars:  $5.3\sigma$  tension between early- and late-Universe probes. *Mon. Not. R. Astron. Soc.* **2019**, *498*, 1420–1439. [[CrossRef](#)]
122. Shajib, A.J.; Birrer, S.; Treu, T.; Agnello, A.; Buckley-Geer, E.J.; Chan, J.H.H.; Christensen, L.; Lemon, C.; Lin, H.; Millon, M.; et al. STRIDES: A 3.9 per cent measurement of the Hubble constant from the strong lens system DES J0408-5354. *Mon. Not. R. Astron. Soc.* **2020**, *494*, 6072–6102. [[CrossRef](#)]
123. Yuan, W.; Riess, A.G.; Macri, L.M.; Casertano, S.; Scolnic, D.M. Consistent Calibration of the Tip of the Red Giant Branch in the Large Magellanic Cloud on the Hubble Space Telescope Photometric System and a Re-determination of the Hubble Constant. *Astrophys. J.* **2019**, *886*, 61. [[CrossRef](#)]
124. Huang, C.D.; Riess, A.G.; Yuan, W.; Macri, L.M.; Zakamska, N.L.; Casertano, S.; Whitelock, P.A.; Hoffmann, S.L.; Filippenko, A.V.; Scolnic, D. Hubble Space Telescope Observations of Mira Variables in the SN Ia Host NGC 1559: An Alternative Candle to Measure the Hubble Constant. *Astrophys. J.* **2020**, *889*, 5. [[CrossRef](#)]
125. Reid, M.J.; Pesce, D.W.; Riess, A.G. An Improved Distance to NGC 4258 and Its Implications for the Hubble Constant. *Astrophys. J.* **2019**, *886*, L27. [[CrossRef](#)]
126. Zhang, P.; D'Amico, G.; Senatore, L.; Zhao, C.; Cai, Y. BOSS Correlation Function analysis from the Effective Field Theory of Large-Scale Structure. *J. Cosmol. Astropart. Phys.* **2022**, *2022*, 036. [[CrossRef](#)]
127. Wang, Y.; Xu, L.; Zhao, G.B. A Measurement of the Hubble Constant Using Galaxy Redshift Surveys. *Astrophys. J.* **2017**, *849*, 84. [[CrossRef](#)]
128. Farren, G.S.; Philcox, O.H.; Sherwin, B.D. Determining the Hubble constant without the sound horizon: Perspectives with future galaxy surveys. *Phys. Rev. D* **2022**, *105*, 063503. [[CrossRef](#)]

129. Philcox, O.H.; Sherwin, B.D.; Farren, G.S.; Baxter, E.J. Determining the Hubble constant without the sound horizon: Measurements from galaxy surveys. *Phys. Rev. D* **2021**, *103*, 023538. [[CrossRef](#)]
130. Anand, G.S.; Tully, R.B.; Rizzi, L.; Riess, A.G.; Yuan, W. Comparing Tip of the Red Giant Branch Distance Scales: An Independent Reduction of the Carnegie-Chicago Hubble Program and the Value of the Hubble Constant. *Astrophys. J.* **2022**, *932*, 15. [[CrossRef](#)]
131. de Jaeger, T.; Galbany, L.; Riess, A.G.; Stahl, B.E.; Shappee, B.J.; Filippenko, A.V.; Zheng, W. A 5% measurement of the Hubble constant from Type II supernovae. *Mon. Not. R. Astron. Soc.* **2022**, *514*, 4620–4628. [[CrossRef](#)]
132. Denzel, P.; Coles, J.P.; Saha, P.; Williams, L.L.R. The Hubble constant from eight time-delay galaxy lenses. *Mon. Not. R. Astron. Soc.* **2020**, *501*, 784–801. [[CrossRef](#)]
133. Chen, G.C.F.; Fassnacht, C.D.; Suyu, S.H.; Rusu, C.E.; Chan, J.H.H.; Wong, K.C.; Auger, M.W.; Hilbert, S.; Bonvin, V.; Birrer, S.; et al. A SHARP view of H0LiCOW: H0 from three time-delay gravitational lens systems with adaptive optics imaging. *Mon. Not. R. Astron. Soc.* **2019**, *490*, 1743–1773. [[CrossRef](#)]
134. Mukherjee, S.; Krolewski, A.; Wandelt, B.D.; Silk, J. Cross-correlating dark sirens and galaxies: Measurement of  $H_0$  from GWTC-3 of LIGO-Virgo-KAGRA. *arXiv* **2022**, arXiv:2203.03643. [[CrossRef](#)]
135. The LIGO Scientific Collaboration; The Virgo Collaboration; The KAGRA Collaboration; Abbott, R.; Abe, H.; Acernese, F.; Ackley, K.; Adhikari, N.; Adhikari, R.X.; Adkins, V.K.; et al. Constraints on the cosmic expansion history from GWTC-3. *arXiv* **2021**, arXiv:2111.03604. [[CrossRef](#)]
136. Gayathri, V.; Healy, J.; Lange, J.; O'Brien, B.; Szczepanczyk, M.; Bartos, I.; Campanelli, M.; Klimentko, S.; Lousto, C.; O'Shaughnessy, R. Hubble Constant Measurement with GW190521 as an Eccentric Black Hole Merger. *arXiv* **2020**, arXiv:2009.14247. [[CrossRef](#)]
137. Pesce, D.W.; Braatz, J.A.; Reid, M.J.; Riess, A.G.; Scolnic, D.; Condon, J.J.; Gao, F.; Henkel, C.; Impellizzeri, C.M.V.; Kuo, C.Y.; et al. The Megamaser Cosmology Project. XIII. Combined Hubble Constant Constraints. *Astrophys. J.* **2020**, *891*, L1. [[CrossRef](#)]
138. Kourkchi, E.; Tully, R.B.; Anand, G.S.; Courtois, H.M.; Dupuy, A.; Neill, J.D.; Rizzi, L.; Seibert, M. Cosmicflows-4: The Calibration of Optical and Infrared Tully—Fisher Relations. *Astrophys. J.* **2020**, *896*, 3. [[CrossRef](#)]
139. Blakeslee, J.P.; Jensen, J.B.; Ma, C.P.; Milne, P.A.; Greene, J.E. The Hubble Constant from Infrared Surface Brightness Fluctuation Distances. *Astrophys. J.* **2021**, *911*, 65. [[CrossRef](#)]
140. Dialektopoulos, K.F.; Borka, D.; Capozziello, S.; Borka Jovanović, V.; Jovanović, P. Constraining nonlocal gravity by S2 star orbits. *Phys. Rev. D* **2019**, *99*, 044053.
141. Bouchè, F.; Capozziello, S.; Salzano, V.; Umetsu, K. Testing non-local gravity by clusters of galaxies. *Eur. Phys. J. C* **2022**, *82*, 652.
142. Capozziello, S.; De Ritis, R.; Rubano, C.; Scudellaro, P. Noether symmetries in cosmology. *La Rivista del Nuovo Cimento* **1996**, *19N4*, 1–114. [[CrossRef](#)]
143. Capozziello, S.; D'Agostino, R.; Luongo, O. The phase-space view of non-local gravity cosmology. *Phys. Lett. B* **2022**, *834*, 137475.
144. Capozziello, S.; Lambiase, G. PeV IceCube signals and  $H_0$  tension in the framework of Non-Local Gravity. *arXiv* **2022**, arXiv:2206.03690. [[CrossRef](#)]
145. Dialektopoulos, K.F.; Capozziello, S. Noether symmetries as a geometric criterion to select theories of gravity. *Int. J. Geom. Methods Mod. Phys.* **2018**, *15*, 1840007. [[CrossRef](#)]
146. Gillessen, S.; Eisenhauer, F.; Trippe, S.; Alexander, T.; Genzel, R.; Martins, F.; Ott, T. Monitoring stellar orbits around the massive black hole in the galactic centre. *Astrophys. J.* **2009**, *692*, 1075. [[CrossRef](#)]
147. Postman, M.; Coe, D.; Benítez, N.; Bradley, L.; Broadhurst, T.; Donahue, M.; Ford, H.; Graur, O.; Graves, G.; Jouvel, S.; et al. The Cluster Lensing And Supernova survey with Hubble: An overview. *Astrophys. J. Suppl. Ser.* **2012**, *199*, 25. [[CrossRef](#)]
148. Umetsu, K.; Zitrin, A.; Gruen, D.; Merten, J.; Donahue, M.; Postman, M. CLASH: Joint analysis of strong-lensing, weak-lensing shear, and magnification data for 20 galaxy clusters. *Astrophys. J.* **2016**, *821*, 116. [[CrossRef](#)]
149. Burstein, D.; Bender, R.; Faber, S.; Nolthenius, R. Global Relationships Among the Physical Properties of Stellar Systems. *Astron. J.* **1997**, *114*. [[CrossRef](#)]
150. Belgacem, E.; Finke, A.; Frassino, A.; Maggiore, M. Testing nonlocal gravity with Lunar Laser Ranging. *J. Cosmol. Astropart. Phys.* **2019**, *2019*, 35. [[CrossRef](#)]
151. Vainshtein, A. To the problem of nonvanishing gravitation mass. *Phys. Lett. B* **1972**, *39*, 393–394. [[CrossRef](#)]
152. Belgacem, E.; Dirian, Y.; Foffa, S.; Maggiore, M. Gravitational-wave luminosity distance in modified gravity theories. *Phys. Rev. D* **2018**, *97*, 104066. [[CrossRef](#)]
153. Belgacem, E.; Dirian, Y.; Foffa, S.; Maggiore, M. Modified gravitational-wave propagation and standard sirens. *Phys. Rev. D* **2018**, *98*, 023510. [[CrossRef](#)]
154. Abbott, B.P.; Abbott, R.; Abbott, T.D.; Acernese, F.; Ackley, K.; Adams, C.; Adams, T.; Addesso, P.; Adhikari, R.X.; Adya, V.B.; et al. Gravitational Waves and Gamma-Rays from a Binary Neutron Star Merger: GW170817 and GRB 170817A. *Astrophys. J.* **2017**, *848*, L13. [[CrossRef](#)]

**Disclaimer/Publisher's Note:** The statements, opinions and data contained in all publications are solely those of the individual author(s) and contributor(s) and not of MDPI and/or the editor(s). MDPI and/or the editor(s) disclaim responsibility for any injury to people or property resulting from any ideas, methods, instructions or products referred to in the content.